Hindawi
Advances in Civil Engineering
Volume 2018, Article ID 5712403, 7 pages
https://doi.org/10.1155/2018/5712403

Research Article

Surface Morphology of Structural Plane and Effects of the Shear Strength Parameters

Dongliang He,[1,2] **Weijun Yang**,[1] **and Yanhui Cheng**[1,2]

[1]*School of Civil Engineering, Changsha University of Science and Technology, Changsha 410114, China*
[2]*School of Civil Engineering, Hunan University of City, Yiyang, Hunan 413000, China*

Correspondence should be addressed to Dongliang He; hedongliang14@126.com

Received 5 June 2018; Accepted 9 August 2018; Published 2 September 2018

Academic Editor: Dan Ma

The surface morphology of a discontinuous structural plane in a natural rock mass is irregular. In studies on the shear strength of discontinuous structural planes, Barton introduced the joint roughness coefficient (JRC) to describe and calibrate the morphological characteristics of a rough structural plane. To describe Barton's typical rough profile model, researchers commonly conduct a comparison based on a standard curve. This approach does not guarantee graphic precision. With subjective comparison reference drawing, the size and angle of a structural plane cannot be quantitatively controlled, and small bumps cannot be described. When the influence of the roughness coefficient of a rock surface is discussed, errors are caused by comparing Barton's typical roughness profile model and a general structural surface model. This paper proposed a new method to simulate Barton's typical structural surface. A numerical model of a complex structural plane is built automatically. The effects of cohesion and internal friction angle on the shear strength of the structural plane are discussed by changing the value of the shear strength parameters.

1. Introduction

A discontinuous structural plane, such as rock joints and fractures, is an important rock mass component that is an essential reason why a rock mass, as an engineering medium, has different characteristics from other engineering media [1–3]. The existence of a structural plane damages the continuity and integrity of a rock mass, causes a rock mass to have unevenness and anisotropy, and greatly reduces the strength and stability of an engineering rock mass [4–11]. In practical engineering, the surface morphology of a discontinuous structural plane in a natural rock mass is irregular [12–14]. Therefore, the shear strength and deformation behavior of a rock structural plane with complex undulations should be investigated. Fan et al. [12] calculated the morphology parameters of the rock joint surface by means of a three-dimensional laser scanning machine. Singh and Basu [15] tried to explore shear behaviors of real' natural unmatching joints (with similar averaged joint roughness coefficients). Belem et al. [16] proposed two surface roughness parameters, joint interface specific surface roughness coefficient SR for quantifying the amount of "pure" roughness and degree of joint interface relative surface roughness DR. In studies on the shear strength of discontinuous structural planes, Barton introduced the joint roughness coefficient (JRC) to describe and calibrate the morphological characteristics of a rough structural plane [14, 17–19]. JRC is the roughness coefficient of a discontinuous surface, and its value is in the range of 0–20. This parameter can be determined by comparing the reference graph of a typical discontinuous plane profile with that of a rough discontinuous surface [20–23]. Du et al. [24] proposed the concepts of rate of JRC scale effect and effective length of JRC scale effect, based on the validity analysis of JRC scale effect. Liu et al. [25] conducted three-dimensional morphology scanning tests and direct shear tests to establish a new peak shear strength criterion. To describe Barton's typical rough profile model, researchers commonly conduct a comparison based on a standard curve. This simple and direct method can ensure that the contour curve of

a structural surface has the morphological characteristics of a standard curve with a low precision. However, this approach does not guarantee graphic precision. With subjective comparison reference drawing, the size and angle of a structural plane cannot be quantitatively controlled, and small bumps cannot be described. Similarities between a simulated curve and an original rough profile curve are inevitably reduced, and the mechanical characteristics cannot be revealed in the subsequent calculation. When the influence of the roughness coefficient of a rock surface is discussed, errors are caused by comparing Barton's typical roughness profile model and a general structural surface model. Previous studies on the shear strength of structural surfaces were usually based on physical experiments and theoretical derivations. With the rapid development of computer technology, a large number of computing capacities of a computer have been applied in civil engineering to solve geotechnical engineering problems [26–32]. Considering the shortcomings of traditional simulation methods, we propose a new method to simulate Barton's typical structural surface. A numerical model of a complex structural plane is built automatically with FLAC3D. The effects of cohesion and internal friction angle on the shear strength of the structural plane are discussed by changing the value of the shear strength parameters in the structural plane.

2. Numerical Model

Two typical rough sections of Barton's curve are selected and named J1 and J2 (Figure 1). The picture is changed into a grayscale map by using MATLAB. The image information is converted into binary point storage, that is, the black part is represented by 1, the white part is represented by 0, and the interception part is signaled. These binary points are precisely processed and numbered to become ordered coordinate points, thereby creating a typical JRC reference curve. Thus, it can be described by discrete coordinate points. When numerous coordinate points exist, the drawn curve becomes close to the real graph. However, too many coordinate points increase the difficulty in dividing a grid. As such, difficulties in dividing the grid and building the required numerical model are encountered. The time of numerical calculation is also greatly prolonged, thereby complicating the calculation. Therefore, 40 points are selected through a trial calculation to describe the JRC curve in this paper to generate the profile curve of a one-dimensional structural plane. The resulting profile curve is then imported into Ansys to build a 3D structural plane model, and the solid unit is cut to create a 3D solid model of the structural plane. Finally, the numerical calculation model was established in FLAC3D (Figure 2). The JRC values of the two models are 9 and 19, respectively. The model size is 10 cm × 10 cm × 10 cm. The physical parameter of rocks is set to an elastic modulus of 2.0 GPa, Poisson's ratio of 0.2, a cohesion of 500 kPa, a bulk density of 23.0 kN/m^3, a dilation angle of 20°, a friction angle of 40°, and a tensile strength of 0.4 MPa. The failure criterion used for the structural plane is the Mohr–Coulomb criterion, and the

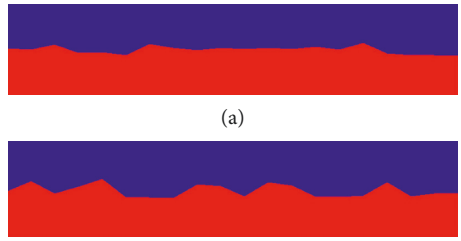

(a)

(b)

Figure 1: Rock structural plane models that differ in roughness. (a) J1 and (b) J2.

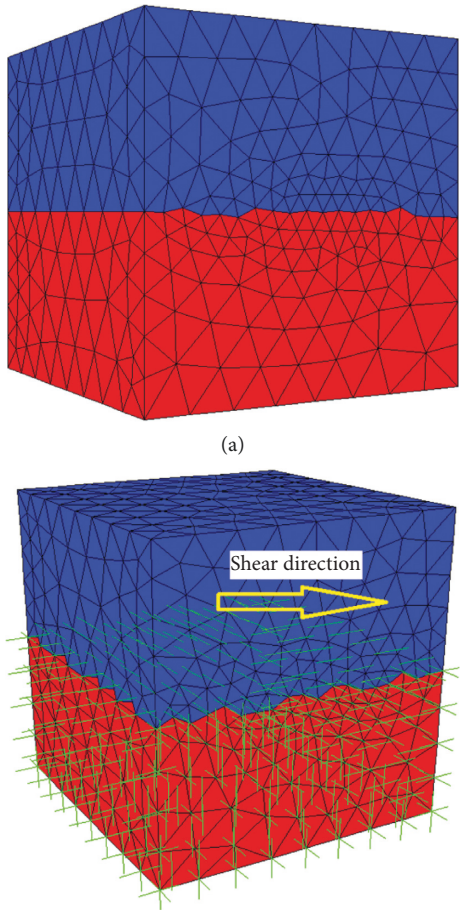

(a)

(b)

Figure 2: Numerical model of the structural plane. (a) J1 and (b) J2.

parameters are as follows: cohesion of 50.0 kPa, internal friction angle of 20°, normal stiffness of 10.0 GPa/m, and shear stiffness of 10.0 GPa. During the direct shear test, the normal stress of the structural plane is set as different values, and the shear velocity is 1.0×10^{-6} mm/step.

3. Analysis of the Influence of Shear Strength Parameters

3.1. Effect of Cohesion on Shear Strength. Figure 3 shows the relationship between the cohesion and shear strength of the

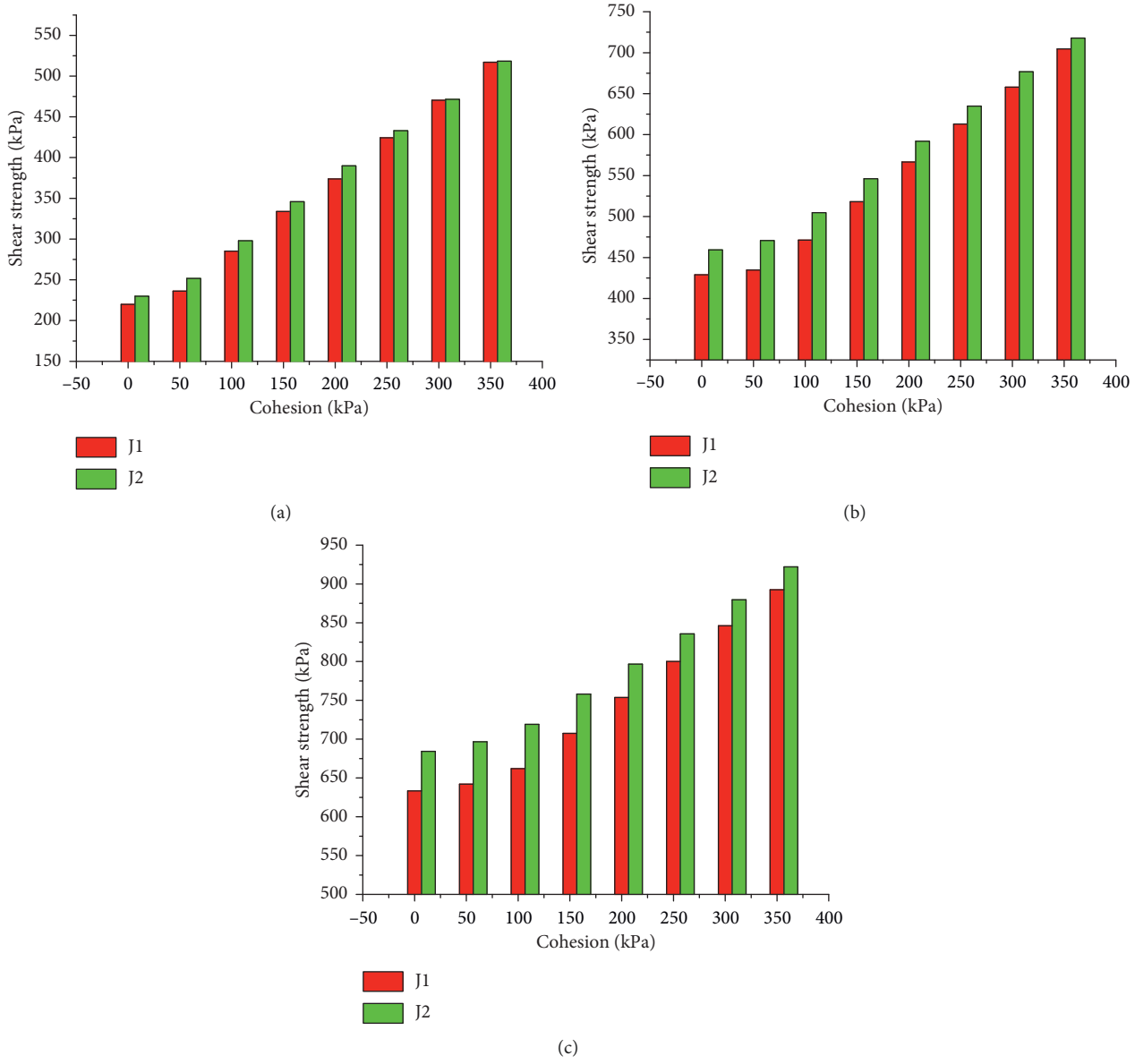

Figure 3: Relationship between the cohesion and the shear strength of the structural planes under different normal stress conditions. (a) Normal stress of 0.5 MPa, (b) normal stress of 1.0 MPa, and (c) normal stress of 1.5 MPa.

structural plane under different normal loads. The shear strength of the structural plane increases as cohesion increases, and the two parameters show certain nonlinear characteristics with small cohesion. As the cohesion of the structural plane increases, the relationship between the two gradually becomes linear. The corresponding shear strength of J2 is greater than that of J1 because the roughness of the former is larger than that of the latter. However, the two slightly differ when the normal stress of the structural surface is low (e.g., 0.5 MPa). As the normal stress of the structure increases (e.g., 1.0 and 1.5 MPa), the difference between the shear strengths of the two increases gradually because the greater the normal stress is, the better the structural plane occlusion is; thus, the corresponding shear strength is largely affected by the roughness of the structural plane. In other words, the greater the normal stress of the structural plane is, the greater the contribution of roughness to shear strength is. When cohesion is low, the shear strengths of J1 and J2 vary greatly. As cohesion increases, the difference in the shear strengths of the two decreases gradually because the roughness of the structural plane is mainly observed in increasing the frictional effect of the structural plane. A high cohesion reduces the influence degree of roughness.

Figure 4 shows the relationship between the normal stress and the shear strengths of J1 and J2. As the normal stress increases, the shear strength of the structural plane increases, and the two have a significant linear relationship, which conforms to the linear characteristics of the Mohr–Coulomb criterion. Thus, the Mohr–Coulomb linear

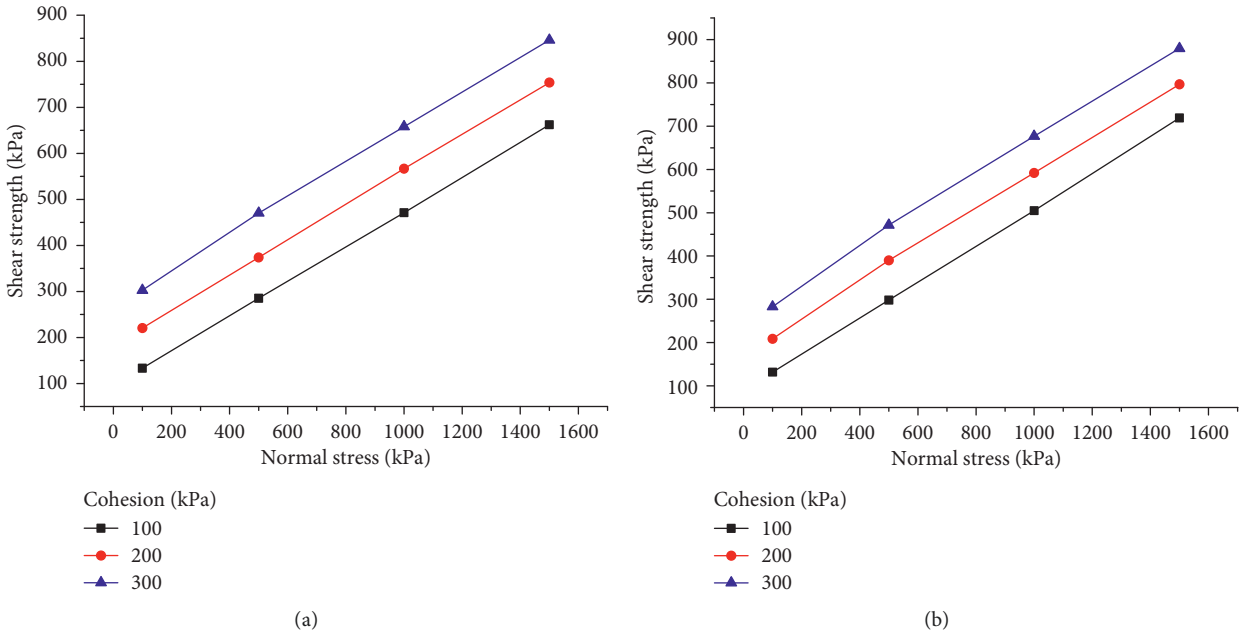

Figure 4: Relationship between normal stress and shear strength. (a) J1 and (b) J2.

equation ($\tau_c = c + \sigma \tan \phi$) can be used to fit these curves (Figure 5). As cohesion increases, the corresponding cohesion and friction angle obtained by fitting also increase. In J1 and J2, the cohesion obtained through fitting calculation is smaller than the set cohesion, and the friction angle is larger than the set friction angle because the cohesion is involved in the friction effect of a part of the structural plane, thereby reducing the cohesive force. The friction effect also includes roughness effect because of the influence of roughness fluctuation. Thus, the internal friction angle of the structural plane increases. Comparing the cohesion and friction angles of J1 and J2 structural planes, we find that the fitting cohesion of J1 is greater than that of J2, indicating that the larger the roughness is, the larger the amount of the adhesive force consumed in the friction process is, resulting in less cohesive force. Therefore, the fitting friction angle of J2 is greater than that of J1.

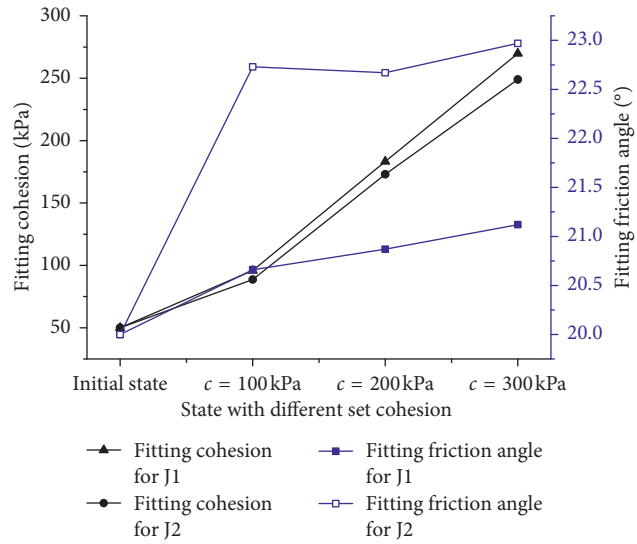

Figure 5: Fitting of the relationship between normal stress and shear strength.

3.2. Effect of Internal Friction Angle on Shear Strength. Figure 6 shows the relationship between the internal friction angle and the shear strength of the structural planes under different normal stress conditions. As the internal friction angle of the structural plane increases, the shear strength also increases gradually, that is, the shear strength of the rock structural plane model presents a monotonous increasing trend as the internal friction angle increases. When the internal friction angle is less than 10°, the shear strength of the structural plane with different roughness values is almost the same. This finding indicates that the influence of roughness on shear strength is not obvious when the internal friction angle is small because when the internal friction angle is small, the structural plane is relatively smooth, the friction effect is low, the shear strength is mainly contributed by the cohesion, and the effect of roughness on the strength of the smooth structural plane is very small. However, when the angle of internal friction is more than 10°, JRC greatly influences the shear strength of the structural plane, suggesting that the frictional effect of the structural surface gradually plays a role when the internal friction angle is larger. Therefore, the frictional effect contributed by roughness also increases gradually, leading to the difference in the shear strengths of J1 and J2. Overall, as the internal friction angle increases, the influence of internal friction angle on shear strength is enhanced, and the effect of the roughness of the structural plane on shear strength is also improved.

Figure 7 illustrates the relationship between the normal stress and the shear strengths of J1 and J2. As the normal

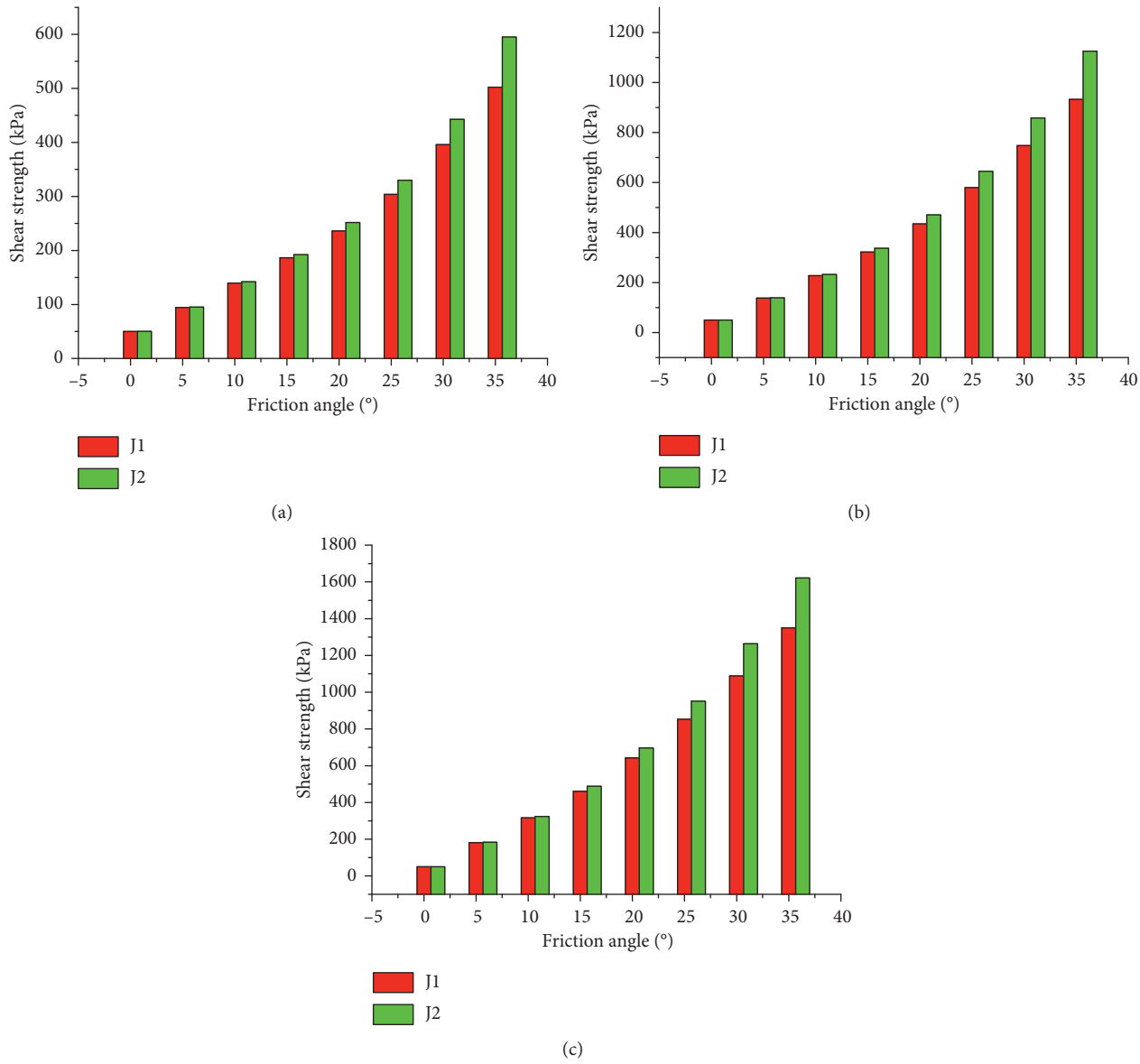

Figure 6: Relationship between the internal friction angle and the shear strength of the structural planes under different normal stress conditions. (a) Normal stress of 0.5 MPa, (b) normal stress of 1.0 MPa, and (c) normal stress of 1.5 MPa.

stress increases, the shear strength of the structural plane increases. Unlike the case of cohesion, the curves are unparallel. The normal stress and the shear strength of the structural plane have a significant linear relationship, which conforms to the linear characteristics of the Mohr–Coulomb criterion. Therefore, these curves can be fitted by using the Mohr–Coulomb linear equation, and Figure 8 is obtained. As the internal friction angle of the structural plane increases, the fitted internal friction angle also increases. When the internal friction angle is small, the fitting internal friction angle is very close to the set friction angle (e.g., $\varphi = 5^{\circ}$–15°) because the surface of the structural plane is relatively smooth, and the effect of roughness on the frictional effect cannot be detected. However, as the internal friction angle increases, the influence of roughness becomes gradually obvious, so the fitting internal friction angle is larger than the set internal friction angle. As the internal friction angle of the structural plane increases, the difference between the fitting internal friction angle and the set internal friction angle also increases, that is, the contribution of roughness becomes increasingly evident. Although the cohesion of the structural plane is set to 50 kPa during calculation, the fitting results show that as the friction angle in the structural plane increases, the fitting cohesion initially decreases and then increases. When the internal friction angle of the structural plane is small, the setting cohesion and the fitting cohesion slightly vary. However, the difference between the two increases as the friction angle in the structural plane increases. The fitting angle of J2 is greater than that of J1 because the roughness of J2 is greater than that of J1.

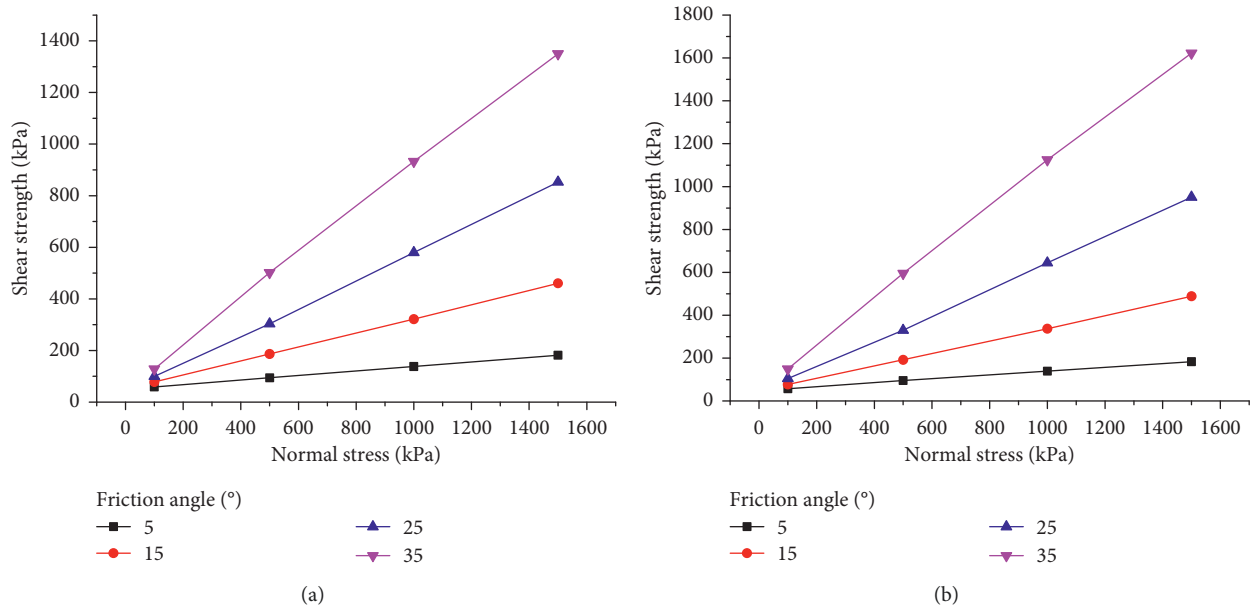

Figure 7: Relationship between normal stress and shear strength. (a) J1 and (b) J2.

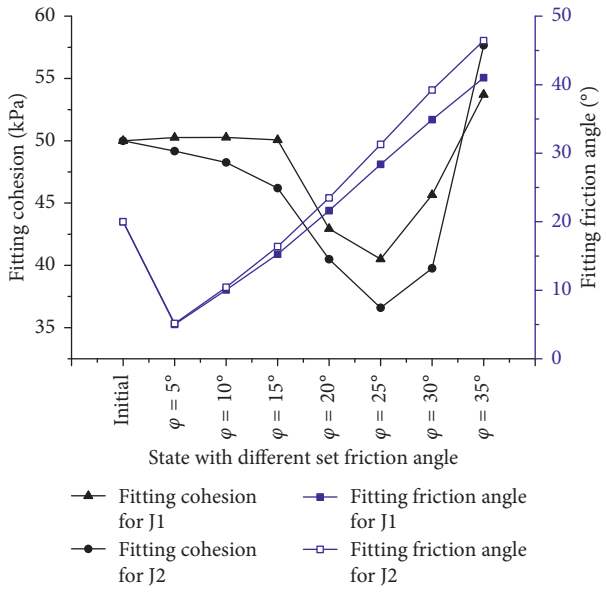

Figure 8: Fitting curve of the relationship between normal stress and shear strength.

4. Conclusions

(1) A numerical model of a complex structural plane is built automatically, which reduced the errors caused by comparing Barton's typical roughness profile model and a general structural surface model.

(2) The shear strength of the structural plane increases as cohesion increases, and the two parameters show certain nonlinear characteristics with small cohesion. As cohesion increases, the corresponding cohesion and friction angle obtained by fitting also increase.

(3) As the internal friction angle of the structural plane increases, the fitted internal friction angle also increases. When the internal friction angle is small, the fitting internal friction angle is very close to the set friction angle.

Data Availability

The data used to support the findings of this study are available from the corresponding author upon request.

Conflicts of Interest

The authors declare that they have no conflicts of interest.

References

[1] Y. L. Zhao, Y. X. Wang, W. J. Wang, W. Wan, and J. Z. Tang, "Modeling of non-linear rheological behavior of hard rock using triaxial rheological experiment," *International Journal of Rock Mechanics and Mining Sciences*, vol. 93, pp. 66–75, 2017.

[2] Y. Zhao, J. Tang, Y. Chen et al., "Hydromechanical coupling tests for mechanical and permeability characteristics of fractured limestone in complete stress-strain process," *Environmental Earth Sciences*, vol. 76, p. 24, 2017.

[3] G. Grasselli, "3D Behaviour of bolted rock joints: experimental and numerical study," *International Journal of Rock Mechanics and Mining Sciences*, vol. 42, no. 1, pp. 13–24, 2005.

[4] H. W. Zhang, Z. Wan, D. Ma, Y. Zhang, J. Cheng, and Q. Zhang, "Experimental investigation on the strength and failure behavior of coal and synthetic materials under plane-strain biaxial compression," *Energies*, vol. 10, no. 4, p. 500, 2017.

[5] R. Cao, W. Tang, H. Lin, and X. Fan, "Numerical analysis for the progressive failure of binary-medium interface under shearing," *Advances in Civil Engineering*, vol. 2018, Article ID 4197172, 11 pages, 2018.

[6] D. Ma, Q. Li, M. R. Hall, and Y. Wu, "Experimental investigation of stress rate and grain size on gas seepage characteristics of granular coal," *Energies*, vol. 10, no. 4, p. 527, 2017.

[7] M. H. Mehranpour and P. H. S. W. Kulatilake, "Improvements for the smooth joint contact model of the particle flow code and its applications," *Computers and Geotechnics*, vol. 87, pp. 163–177, 2017.

[8] W. Wan, J. Liu, and J. Liu, "Effects of asperity angle and infill thickness on shear characteristics under constant normal load conditions," *Geotechnical and Geological Engineering*, vol. 36, no. 4, pp. 2761–2767, 2018.

[9] Y. Zhao, L. Zhang, W. Wang, J. Tang, H. Lin, and W. Wan, "Transient pulse test and morphological analysis of single rock fractures," *International Journal of Rock Mechanics and Mining Sciences*, vol. 91, pp. 139–154, 2017.

[10] Y. Wang, P. P. Guo, W. X. Ren et al., "Laboratory investigation on strength characteristics of expansive soil treated with jute fiber reinforcement," *International Journal of Geomechanics*, vol. 17, no. 11, article 04017101, 2017.

[11] Y. X. Wang, P. P. Guo, F. Dai, X. Li, Y. L. Zhao, and Y. Liu, "Behaviour and modelling of fiber reinforced clay under triaxial compression by using the combining superposition method with the energy based homogenization technique," *International Journal of Geomechanics*, vol. 17, article 04017101, 2017.

[12] W. C. Fan, P. Cao, and L. Long, "Degradation of joint surface morphology, shear behavior and closure characteristics during cyclic loading," *Journal of Central South University*, vol. 25, no. 3, pp. 653–661, 2018.

[13] J. Y. Huang, S. L. Xu, and S. S. Hu, "Numerical investigations of the dynamic shear behavior of rough rock joints," *Rock Mechanics and Rock Engineering*, vol. 47, no. 5, pp. 1727–1743, 2014.

[14] A. Ozvan, I. Dincer, A. Acar, and B. Ozvan, "The effects of discontinuity surface roughness on the shear strength of weathered granite joints," *Bulletin of Engineering Geology and the Environment*, vol. 73, no. 3, pp. 801–813, 2014.

[15] H. K. Singh and A. Basu, "Shear behaviors of 'real' natural unmatching joints of granite with equivalent joint roughness coefficients," *Engineering Geology*, vol. 211, pp. 120–134, 2016.

[16] T. Belem, M. Souley, and F. Homand, "Method for quantification of wear of sheared joint walls based on surface morphology," *Rock Mechanics and Rock Engineering*, vol. 42, no. 6, pp. 883–910, 2009.

[17] N. Barton, "Shear strength criteria for rock, rock joints, rockfill and rock masses: problems and some solutions," *Journal of Rock Mechanics and Geotechnical Engineering*, vol. 5, no. 4, pp. 249–261, 2013.

[18] N. Barton, "Non-linear shear strength for rock, rock joints, rockfill and interfaces," *Innovative Infrastructure Solutions*, vol. 1, p. 30, 2016.

[19] N. Barton and E. F. de Quadros, "Joint aperture and roughness in the prediction of flow and groutability of rock masses," *International Journal of Rock Mechanics and Mining Sciences*, vol. 34, no. 3-4, pp. 252.e1–252.e14, 1997.

[20] B. S. A. Tatone and G. Grasselli, "A new 2D discontinuity roughness parameter and its correlation with JRC," *International Journal of Rock Mechanics and Mining Sciences*, vol. 47, no. 8, pp. 1391–1400, 2010.

[21] P. Asadollahi and F. Tonon, "Constitutive model for rock fractures: revisiting Barton's empirical model," *Engineering Geology*, vol. 113, no. 1–4, pp. 11–32, 2010.

[22] M. Wang, P. Cao, and Y. Chen, "Anisotropy of rock profile JRC values and its empirical formula: a case study on yellow rust granite," *Geotechnical and Geological Engineering*, vol. 35, no. 4, pp. 1645–1655, 2017.

[23] H. Lin, Z. Xiong, T. Liu, R. Cao, and P. Cao, "Numerical simulations of the effect of bolt inclination on the shear strength of rock joints," *International Journal of Rock Mechanics and Mining Sciences*, vol. 66, pp. 49–56, 2014.

[24] S. G. Du, H. C. Gao, Y. J. Hu, M. Huang, and H. Zhao, "A new method for determination of joint roughness coefficient of rock joints," *Mathematical Problems in Engineering*, vol. 2015, Article ID 634573, 6 pages, 2015.

[25] Q. S. Liu, Y. C. Tian, P. Q. Ji, and H. Ma, "Experimental investigation of the peak shear strength criterion based on three-dimensional surface description," *Rock Mechanics and Rock Engineering*, vol. 51, no. 4, pp. 1005–1025, 2018.

[26] H. Lin, H. Wang, X. Fan, P. Cao, and K. Zhou, "Particle size distribution effects on deformation properties of graded aggregate base under cyclic loading," *European Journal of Environmental and Civil Engineering*, pp. 1–18, 2017.

[27] R. Cao, P. Cao, H. Lin, and X. Fan, "Experimental and numerical study of the failure process and energy mechanisms of rock-like materials containing cross un-persistent joints under uniaxial compression," *PLoS One*, vol. 12, no. 12, Article ID e0188646, 2017.

[28] S. Q. Yang, T. Xu, L. He, H. W. Jing, S. Wen, and Q. L. Yu, "Numerical study on failure behavior of brittle rock specimen containing pre-existing combined flaws under different confining pressure," *Archives of Civil and Mechanical Engineering*, vol. 15, no. 4, pp. 1085–1097, 2015.

[29] K. Zhao, M. Janutolo, G. Barla, and G. Chen, "3D simulation of TBM excavation in brittle rock associated with fault zones: the brenner exploratory tunnel case," *Engineering Geology*, vol. 181, pp. 93–111, 2014.

[30] R. Hasanpour, "Advance numerical simulation of tunneling by using a double shield TBM," *Computers and Geotechnics*, vol. 57, pp. 37–52, 2014.

[31] M. Bahaaddini, G. Sharrock, and B. K. Hebblewhite, "Numerical direct shear tests to model the shear behaviour of rock joints," *Computers and Geotechnics*, vol. 51, pp. 101–115, 2013.

[32] N. Erarslan and D. J. Williams, "Experimental, numerical and analytical studies on tensile strength of rocks," *International Journal of Rock Mechanics and Mining Sciences*, vol. 49, pp. 21–30, 2012.